Research Article

Nande Mgedle, Olanrewaju A. Aladesuyi, Thabang Calvin Lebepe, Vuyelwa Ncapayi, and Oluwatobi Samuel Oluwafemi*

Facile aqueous synthesis of ZnCuInS/ZnS–ZnS QDs with enhanced photoluminescence lifetime for selective detection of Cu(II) ions

https://doi.org/10.1515/gps-2022-8155
received December 27, 2022; accepted April 20, 2023

Abstract: Quaternary quantum dots (QDs) have recently gained more attention due to their low toxicity, tunable wavelength, reduced or no blueshift emission upon overcoating, improved photoluminescence (PL) quantum yield, and PL lifetime when compared to their binary (II–VI) and ternary (I–III–VI) counterparts. In this work, the aqueous synthesis of ZnCuInS/ZnS–ZnS multi-shell quaternary QDs as a nanosensor for the selective detection of Cu^{2+} ions was reported. The as-synthesized QDs were spherical, with a particle diameter of 3.66 ± 0.81 nm, and emitted in the first near-infrared window (725 nm) with an average decay PL lifetime of 43.69 ns. The X-ray diffraction analysis showed that the QDs were of the wurtzite structure, while the Fourier transform infrared spectroscopy confirmed GSH capping through the sulphur–metal bond. Furthermore, the fluorometric study shows that the developed multi-shell QDs were selective towards Cu^{2+} ions compared to other metal ions via fluorescence quenching with a limit of detection of 1.4 μM, which is below the acceptable limit in drinking water.

Keywords: quantum dots, ZnCuInS/ZnS–ZnS multi-shell, lifetime, emission, absolute quantum yield

1 Introduction

Semiconductor nanocrystals, also known as quantum dots (QDs), have recently received a lot of attention due to their exemplary photoluminescence (PL) properties, such as wide excitation spectra, narrow symmetrical emission spectra, tunable emission wavelengths, high PL quantum yields (PLQYs), and photochemical stabilities [1,2]. Previously, binary (II–VI) QDs have been developed; however, the toxic nature has limited their applications, especially in biological and biomedical fields [3,4]. For this reason, low toxic and biocompatible ternary QDs (I–III–VI), such as CuInS and AgInS, have been proposed [5–14]. Nonetheless, the optical properties of these QDs are not comparable to those of binary QDs. Overcoating ternary QDs with a high bandgap inorganic material, such as ZnS and ZnSe, have been proposed as one of the effective methods to improve the optical properties of ternary QDs [15,16]. Passivated QDs have been reported to exhibit enhanced PLQY and improved intensities due to the removal of surface defects [17]. However, a blueshift in the emission wavelength upon passivation has been reported. This blueshift has been attributed to the interdiffusion of the metal ion (Zn ions) into the surface of the core (e.g., copper indium sulfide [CIS]) [18]. Hence, quaternary (I–II–III–IV) QDs have been developed as an emerging strategy to reduce the blue-shifted emission. This can be achieved, for example, by adding Zn ions with CIS precursor, thus reducing the displacement of Cu^{2+} and In^{3+} ions by the Zn^{2+} ions upon passivation. Jiao et al. [19] observed an enhanced quantum yield of 30.8% for zinc copper indium sulfide (ZCIS)/ZnS core/shell QDs, as against that of the ZCIS core (14.7%). The result showed no blue-shifted emission upon passivation; the quaternary QDs showed tunable emission ranging from

* **Corresponding author: Oluwatobi Samuel Oluwafemi,** Department of Chemical Sciences, University of Johannesburg, P.O. Box 17011, Doornfontein, Johannesburg 2028, South Africa; Centre for Nanomaterials Science Research, University of Johannesburg, P.O. Box 17011, Doornfontein, Johannesburg 2028, South Africa, e-mail: oluwafemi.oluwatobi@gmail.com
Nande Mgedle: Department of Chemical Sciences, University of Johannesburg, P.O. Box 17011, Doornfontein, Johannesburg 2028, South Africa; Centre for Nanomaterials Science Research, University of Johannesburg, P.O. Box 17011, Doornfontein, Johannesburg 2028, South Africa, e-mail: nandemgedle@gmail.com
Olanrewaju A. Aladesuyi, Thabang Calvin Lebepe, Vuyelwa Ncapayi: Department of Chemical Sciences, University of Johannesburg, P.O. Box 17011, Doornfontein, Johannesburg 2028, South Africa; Centre for Nanomaterials Science Research, University of Johannesburg, P.O. Box 17011, Doornfontein, Johannesburg 2028, South Africa

535 to 645 nm. In another development, Zheng et al. [20] synthesized less-toxic quaternary ZnCuInS QDs with tunable emission ranging from 564 to 650 nm. Thus, having such quaternary material with emission in the near-infrared window is highly desirable. Quaternary QDs could be synthesized via organic synthetic routes such as the hot-injection method and hydrothermal techniques. However, these methods involve the use of high reaction temperatures, toxic and expensive chemicals, etc. In addition, the QDs synthesized via organic synthesis methods are hydrophobic in nature, which limits their biological applications. Hence, there is a need for the development of a direct, economically, and environmentally friendlier method. Therefore, in this study, aqueous synthesis was used [21,22].

Water pollution remains a global issue as this have a negative effect on humans and the environment [23–25]. Fluorescent nanoprobes such as QDs have been used as a greener method for detecting various toxic heavy metal ions [26–30]. The concentration of Cu^{2+} in drinking water needs to be highly monitored, especially those distributed using copper pipes, as there is a possibility for the corrosion of copper plumbing [31]. According to the World Health Organization (WHO), the maximum accepted Cu^{2+} ion concentration in drinking water is 1.33 ppm [32]. The consumption of high concentrations of Cu^{2+} ions results in extreme toxicity and a threat to the health and the ecosystem. The long-term risks of Cu^{2+} include diabetes, anaemia, kidney disorders, liver damage, and death [33]. Hence, it is paramount to determine the actual amount of Cu^{2+} ions in solutions.

This study reports for the first time, as far as the authors know, the aqueous synthesis of ZCIS/ZnS–ZnS multi-shell QDs with enhanced PL lifetime, PLQY, and reduced blue-shifted emission after passivation. Herein, we further passivate the single-shell QDs by a second shell to further red shift the emission wavelength and improve the PLQY. The ultraviolet-visible (UV-vis) spectroscopy, PL, Fourier transform infrared spectroscopy (FTIR), X-ray diffraction (XRD), high-resolution transmission electron microscopy (HRTEM), and energy-dispersive spectroscopy (EDS) were used to characterize the as-synthesized ZnCuInS/ZnS–ZnS multi-shell quaternary QDs. The multi-shell QDs were then used for sensing Cu^{2+} via fluorescent quenching. The ZCIS/ZnS–ZnS nanoprobes exhibit a selective detection of Cu^{2+} amidst other interfering metal ions.

2 Materials and methods

2.1 Materials

Iron(III) chloride hexahydrate ($FeCl_3{\cdot}6H_2O$), copper(II) chloride ($CuCl_2$), indium chloride ($InCl_3$), sodium citrate ($Na_3C_6H_5O_7$), L-glutathione reduced (GSH), sodium sulphide (Na_2S), zinc acetate dihydrate ($Zn(O_2CCH_3)_2(H_2O)_2$), thiourea (CH_4N_2S), hydrochloride (HCl), ethanol (CH_3CH_2OH), mercury chloride ($HgCl_2$), cadmium nitrate tetrahydrate ($Cd(NO_3)_2{\cdot}4H_2O$), and nickel(II) chloride hexahydrate ($NiCl_2{\cdot}6H_2O$) were purchased from Sigma Aldrich and used without further purification.

2.2 Synthesis of ZnCuInS/ZnS–ZnS multi-shell QDs

Water-soluble QDs were synthesized using reflux approach by following the method of Tsolekile et al. [3] with slight modifications. In a typical reaction, ZnCuInS/ZnS core/shell QDs were synthesized by adding zinc acetate ($Zn(O_2CCH_3)_2(H_2O)_2$), copper chloride ($CuCl_2$), indium chloride ($InCl_3$), GSH, sodium citrate, and sodium sulphide (Na_2S) precursors followed by reflux for 45 min at 95°C to produce ZnCuInS cores. This was followed by *in situ* passivation with the shell material by adding ($Zn(O_2CCH_3)_2(H_2O)_2$) and thiourea (CH_4N_2S). Furthermore, the reaction was refluxed for 80 min at 95°C to form ZnCuInS/ZnS core/shell QDs. The ZnCuInS/ZnS–ZnS multi-shell QDs were synthesized by cooling the reaction solution containing ZnCuInS/ZnS core/shell QDs to 80°C followed by the second addition of the shell precursors such as zinc acetate ($Zn(O_2CCH_3)_2(H_2O)_2$) and thiourea (CH_4N_2S). The reaction mixture was further refluxed at 95°C for 80 min followed by cooling and purification with ethanol (QDs: 1:3 ethanol). After purification, the mixture was centrifuged, and ZnCuInS/ZnS–ZnS multi-shell QDs were collected.

2.3 Sensing

A method by Muthivhi et al. [34] was followed with slight modifications for the sensing of Cu^{2+} ion. In a typical experiment, 200 µL of ZCIS/ZnS–ZnS multi/shell QDs was added to 2 mL of Cu^{2+} ions at different concentrations from 0 to 10 µM. The resultant mixture was left for 2 min to ensure proper ion interaction and incubation. Thereafter, the PL spectra were recorded at 450 nm excitation wavelength at room temperature. The same procedure was repeated for the selectivity studies. About 10 µM of Hg^{2+}, Co^{2+}, Cd^{2+}, Zn^{2+}, Ni^{2+}, Mg^{2+}, and Fe^{3+} was mixed with 200 µM of the QDs followed by analysis. The selectivity of ZCIS/ZnS–ZnS multi/shell QDs towards Cu^{2+} was further evaluated by repeating the same procedure for a mixture of Cu^{2+} ion with interfering ions of Hg^{2+}, Co^{2+}, Cd^{2+}, Zn^{2+}, Ni^{2+}, Mg^{2+}, and Fe^{3+} ions. In the mixture, the ratio of Cu^{2+} ion to other metal ions was 1:1.

2.4 Characterization

The UV-vis spectra were acquired using Lambda 25, PerkinElmer UV-vis spectrophotometer in the range of 200–700 nm, while the emission, lifetime, and relative QYs were recorded using spectrofluorometer FS5 (Edinburgh instruments). The surface chemistry of the as-synthesized quaternary QDs was analysed using FTIR, while the morphology and elemental composition (EDS) were investigated using HRTEM JEOL 2100 at 200 kV. XRD patterns were obtained using an advanced D8 Bruker X-ray diffractometer with a monochromatic Cu Kα radiation (λ = 0.15406 nm) at room temperature. Scanning was performed at 2θ ranging from 5° to 90° in steps of 0.017°·s^{-1}, with the accelerating voltage and current flux set at 40 kV and 30 mA, respectively.

3 Results and discussion

The absorption spectra showed no excitonic features for ZnCuInS, ZnCuInS/ZnS, and ZnCuInS/ZnS–ZnS QDs (Figure 1a). This could be attributed to the joint effect of broad size distribution, irregular composition distribution, and various intra-bandgap states [22]. The bandgap was recorded to be 3.46, 3.69, and 4.39 eV for ZnCuInS, ZnCuInS/ZnS, and ZnCuInS/ZnS–ZnS QDs, respectively (Table 1). The PL properties of the as-synthesized QDs are shown in Figure 1. The ZnCuInS core, ZnCuInS/ZnS core/shell, and ZnCuInS/ZnS multi-shell QDs showed emission at 725, 720 and 725 nm, respectively (Table 1). The blue-shifted emission after the first shell formation could be attributed to the interdiffusion of Zn ions upon passivation [35]. The multi-shell QDs showed red-shifted emission from the single-shell QDs. The absolute QY of ZnCuInS core, ZnCuInS/ZnS core/shell, and ZnCuInS/ZnS–ZnS multi-shell QDs is 1.28%, 4.11%, and 6.44%, respectively (Table 1). These results indicate that passivation of ZCIS core QDs with the shell material removed surface trap states and suppressed the recombination process (Table 1 and Figure 1b).

Time-resolved PL measurements were carried out to understand the charge carrier lifetime of the synthesized QDs. The decay curve was fitted by bi-exponential fitting, as shown in Figure 2. The average decay lifetime of the as-synthesized ZnCuInS, ZnCuInS/ZnS, and ZnCuInS/ZnS–ZnS multi-shell QDs was found to be 19.81, 35.59, and 43.69 ns,

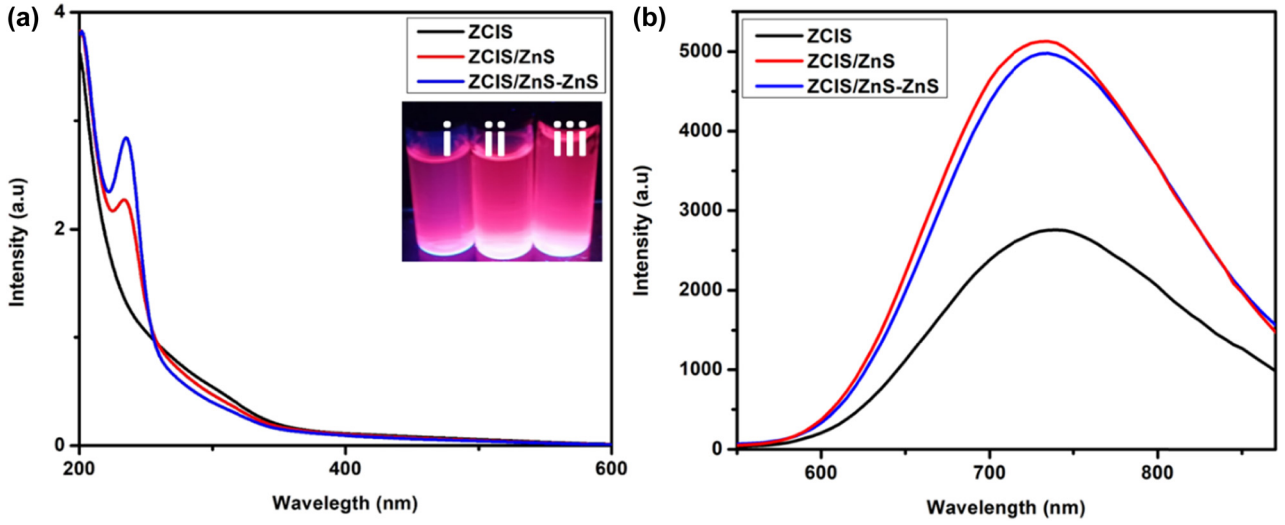

Figure 1: (a) Absorption and (b) PL spectra of ZCIS, ZCIS/ZnS core/shell, and ZCIS/ZnS–ZnS multi-shell QDs.

Table 1: Optical properties of the synthesized QDs

QD	Band gap (eV)	Emission (nm)	PLQY (%)	τ_1 (ns)	τ_2 (ns)	$\tau_{Average}$ (ns)
ZCIS	3.46	725.00	1.28	2.51	37.10	19.81
ZCIS/ZnS	3.69	720.00	4.11	2.59	68.59	35.59
ZCIS/ZnS–ZnS	4.39	725.00	6.44	4.38	82.99	43.69

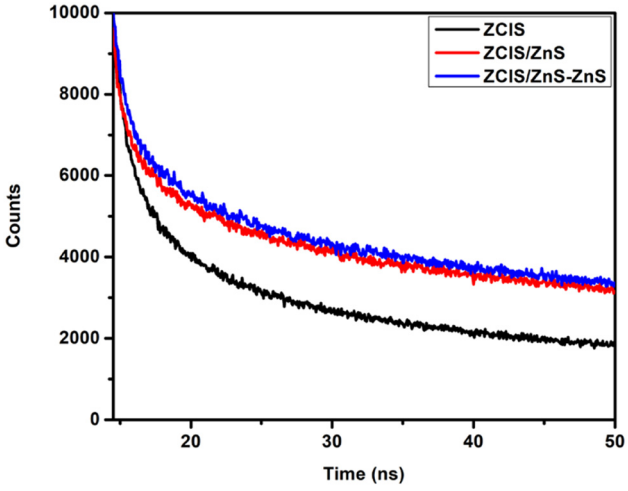

Figure 2: PL lifetime spectra of ZCIS, ZCIS/ZnS core/shell, and ZCIS/ZnS–ZnS multi-shell QDs.

respectively, as shown in Table 1 and Figure 2. This indicates that overcoating QDs with a second ZnS shell further passivates the core and inhibits the structural defects.

The typical FTIR spectra of the as-prepared QDs (Figure 3) showed an –OH peak at around 3,294 cm^{-1}. The characteristics –C═O– and N–H deformation were observed at 1,575 and 1,377 cm^{-1}, respectively. The GSH has –SH– vibrations at around 2,524 cm^{-1}. The absence of this peak indicates that the capping of GSH with QDs occurred through thiol and metal coordination [3,36]. The XRD patterns (Figure 3b) of the ZCIS/ZnS–ZnS multi-shell QDs consist of three distinct peaks at 2θ: 27.93°, 47.06°, and 55.12° corresponding to (112), (204), and (302), which are consistent with those of the zinc blende crystalline planes (JCPDS 05-0566 number) [25,26]. The typical HRTEM analysis (Figure 3c) revealed that the as-synthesized ZCIS/ZnS–ZnS QDs were spherical and mono-dispersed. The particle size

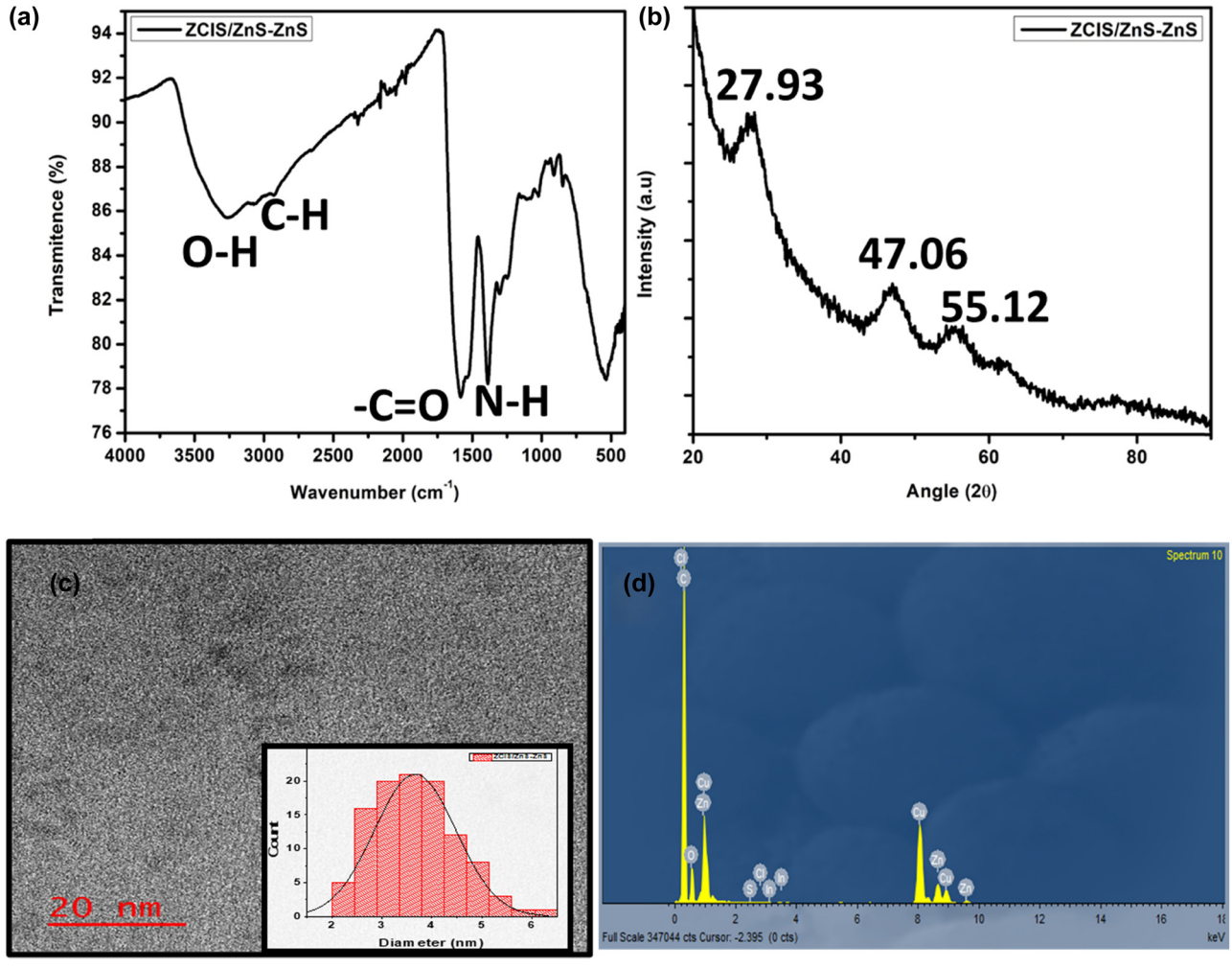

Figure 3: (a) FTIR spectrum of ZCIS/ZnS–ZnS multi-shell QDs; (b) XRD spectrum of ZCIS/ZnS–ZnS multi-shell QDs; (c) HRTEM image of ZCIS/ZnS–ZnS multi-shell QDs, inset size distribution; and (d) EDS spectrum of ZCIS/ZnS–ZnS multi-shell QDs.

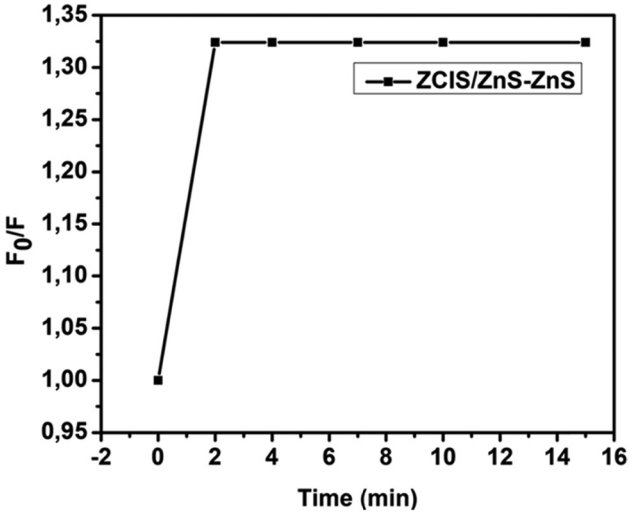

Figure 4: Effects of reaction time on the PL intensity of ZCIS/ZnS–ZnS multi-shell QDs mixed with 0.025 μM Cu^{2+}.

distribution indicates an average size of 3.66 ± 0.81 nm. In addition, the increase in the particle size from 2.97 nm of the core/shell (TEM not shown here) to 3.66 nm of the core/shell/shell and the change in the emission position in Figure 1 suggest the formation of multi-shell QDs. The EDS spectra of the multi-shell quaternary QDs (Figure 3d) show the corresponding elements of the core and the shell material, i.e. Zn, Cu, In, and S. The presence of C and O is ascribed to the capping agent, GSH. In contrast, the sulphur present is ascribed to the GSH and Zn–Cu–In–S QDs.

The sensing of Cu^{2+} was investigated at various incubation times (Figure 4). The fluorescent intensity increases with the incubation time, reaching the maximum at 2 min, and the intensity remains constant even at longer reaction times. Hence, 2 min was chosen as the optimized incubation time for the proper interaction between Cu^{2+} ions and QD.

Table 2: Comparison of Cu^{2+} detection using different nanosensors

Probe	Linear range	LOD	Reference
PEG-ZnS QD@ZIF-67	3–500 nM	0.96 nM	[37]
CdSe/ZnS QD @PESM	10–1,000 μg·L^{-1}	4.27 μg·L^{-1}	[38]
CdTe QDs	0.5–40 ng·mL^{-1}	0.088 ng·mL^{-1}	[39]
APBA-CdTe QDs	0.01–20 μM	7.6 μM	[40]
CIZS/ZnS QDs	0.020–20 μM	6.7 nM	[19]
ZCIS/ ZnS–ZnS QDs	0.025–10 μM	1.4 μM	This work

Different concentrations of Cu^{2+} ions (0.025–10 μM) were also sensed to determine the limit of detection (LOD) (Figure 5). The results showed that an increase in the concentration of Cu^{2+} ions resulted in a decreased fluorescence intensity of the QDs. The quenching behaviour of AIS-ZnS QDs fluorescence by Cu^{2+} ions could be explained using the Stern–Volmer equation, which is as follows:

$$\frac{F_0}{F} = 1 + K_{SV}[C] \quad (1)$$

where F_0 represents the blank QD intensity, F is the QDs with the analyte (Cu^{2+}) fluorescence intensity, K_{SV} is the

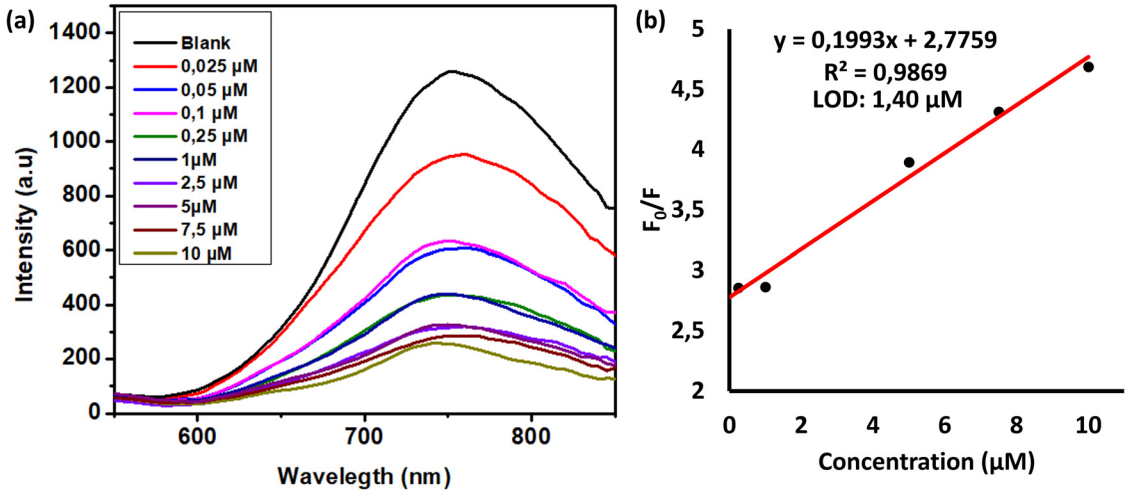

Figure 5: (a) PL spectra of ZCIS/ZnS–ZnS multi-shell QDs at different concentrations of Cu^{2+} ions (0.025–10 μM) and (b) corresponding Stern–Volmer plot (0.5–10 μM).

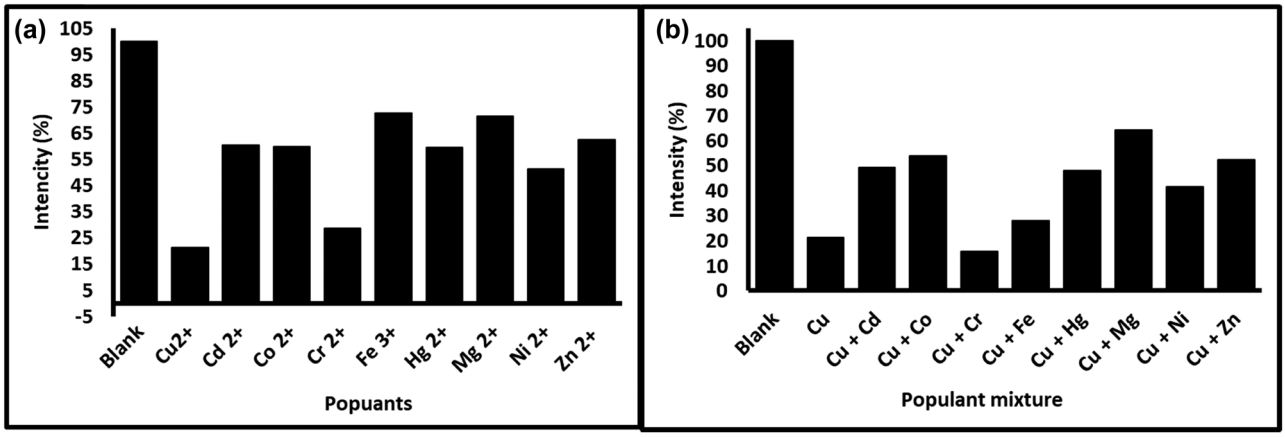

Figure 6: (a) Effect of different metal ions on the intensity of the as-synthesized multi-shell quaternary QDs and (b) selectivity of the multi-shell quaternary QDs towards Cu^{2+} in the presence of other metal ions at a concentration of 10 μM.

Stern–Volmer constant, and *C* is the concentration of the analyte [12].

The LOD for Cu^{2+} was calculated to be 1.4 μM with an R^2 of 0.98 using the relation:

$$\text{LOD} = \frac{(3.3^{*}\text{SD})}{\text{m}} \quad (2)$$

where *SD* is the standard deviation of the blank QDs, and *S* is the slope of the calibration curve [36]. The comparison of the calculated LOD with previous reports is shown in Table 2.

The selectivity study was conducted using 10 μM concentrations of Cu^{2+} and metal ions (Figure 6a). The results showed that Cu^{2+} ions significantly quenched the fluorescence intensity compared to other metal ions. Furthermore, a mixture of Cu^{2+} ions with each of the interfering metal ions was added to the aqueous solution of the QD (Figure 6b). The result showed that the extent of GSH-capped multi-shell QD fluorescence intensity quenching by Cu^{2+} ions was not affected by the presence of other metal ions, thus depicting its selectivity towards Cu^{2+}. The selectivity of ZCIS/ZnS–ZnS multi-shell QDs has been attributed to the strong affinity between Cu^{2+} and the capping molecule GSH, which tends to produce a strong ligand–metal complex more than other metal ions [36].

4 Conclusions

In summary, water-soluble ZCIS/ZnS–ZnS multi-shell quaternary QDs were synthesized. The as-synthesized multi-shell quaternary QDs were spherical in shape with an average particle diameter of 3.66 ± 0.81 nm. The EDS indicated the presence of Zn, Cu, In, and S. However, the FTIR analysis confirmed the GSH capping on the multi-shell quaternary QDs through S-metal bonding. The XRD results confirmed the formation of zinc blende crystalline structure. The absolute QY was improved to 6.14% for ZCIS/ZnS–ZnS multi-shell quaternary QDs compared to ZCIS and ZCIS/ZnS QDs. In addition, the multi-shell quaternary QDs show the highest average optical lifetime of 43.69 ns, making them an ideal material for near-infrared imaging applications. The developed QDs were sensitive and selective towards Cu^{2+} ions amidst other interfering ions with an LOD that is lower than the maximum acceptable concentration (1.33 ppm) by WHO.

Funding information: This work was supported by the National Research Foundation (NRF) under the Competitive Programme for Rated Researchers (CPRR), Grants No. 129290, the University of Johannesburg (URC), and the Faculty of Science (FRC).

Author contributions: Oluwatobi Samuel Oluwafemi: conceptualization, project administration; resources; writing – review and editing, resources; Nande Mgedle: writing – original draft, methodology, formal analysis; Olanrewaju A. Aladesuyi: writing – editing, formal analysis; Vuyelwa Ncapayi: formal analysis; Thabang Calvin Lebepe: formal analysis, visualization.

Conflict of interest: The authors state no conflict of interest.

Data availability statement: The datasets generated and analysed during this study are available from the corresponding author upon a reasonable request.

References

[1] Mbaz GIM, Parani S, Oluwafemi OS. Controlled synthesis of silver-based ternary quantum dots with outstanding luminescence. J Fluoresc. 2022;32:1769–77.

[2] Mbaz GIM, Parani S, Oluwafemi OS. Instant removal of methylene blue using water-soluble non-cadmium based quantum dots. Mater Lett. 2021;303:130495.

[3] Tsolekile N, Parani S, Vuyelwa N, Maluleke R, Matoetoe M, Songca S, et al. Synthesis, structural and fluorescence optimization of ternary Cu–In–S quantum dots passivated with ZnS. J Lumin. 2020;227:117541.

[4] Jose Varghese R, Parani S, Adeyemi OO, Remya VR, Sakho EHM, Maluleke R, et al. Green synthesis of sodium alginate capped -$CuInS_2$ quantum dots with improved fluorescence properties. J Fluoresc. 2020;30:1331–5.

[5] Jose Varghese R, Parani S, Remya VR, Lebepe TC, Maluleke R, Aladesuyi OA, et al. Gelatin stabilized mesoporous silica $CuInS_2$_ZnS nanocomposite as a potential near-infrared probe and their effect on cancer cell lines. J Mater Sci. 2022;57:11911–7.

[6] May BMM, Parani S, Rajendran JV, Oluwafemi OS. Selective detection of folic acid in the midst of other biomolecules using water-soluble $AgInS_2$ quantum dots. MRS Commun. 2019;9:1306–10.

[7] May BMM, Parani S, Oluwafemi OS. Detection of ascorbic acid using green synthesized AgInS2 quantum dots. Mater Lett. 2019;236:432–5.

[8] Oluwafemi OS, May BMM, Parani S, Tsolekile N. Facile, large scale synthesis of water soluble $AgInSe_2$/ZnSe quantum dots and its cell viability assessment on different cell lines. Mater Sci Eng C. 2020;106:110181.

[9] Tsolekile N, Parani S, Matoetoe MC, Songca SP, Oluwafemi OS. Evolution of ternary I–III–VI QDs: Synthesis, characterization and application. Nano-Struct Nano-Objects. 2017;12:46–56.

[10] Zikalala N, Parani S, Tsolekile N, Oluwafemi OS. Facile green synthesis of ZnInS quantum dots: Temporal evolution of their optical properties and cell viability against normal and cancerous cells. J Mater Chem C. 2020;8:9329–36.

[11] Jain S, Bharti S, Bhullar GK, Tripathi SK. I-III-VI core/shell QDs: Synthesis, characterizations and applications. J Lumin. 2020;219:116912.

[12] Parani S, Oluwafemi OS. Selective and sensitive fluorescent nanoprobe based on $AgInS_2$-ZnS quantum dots for the rapid detection of Cr (III) ions in the midst of interfering ions. Nanotechnology. 2020;31:395501.

[13] Xu Y, Chen T, Hu X, Jiang W, Wang L, Jiang W, et al. The off-stoichiometry effect on the optical properties of water-soluble copper indium zinc sulfide quantum dots. J Colloid Interface Sci. 2017;496:479–86.

[14] Jiao M, Li Y, Jia Y, Li C, Bian H, Gao L, et al. Strongly emitting and long-lived silver indium sulfide quantum dots for bioimaging: Insight into co-ligand effect on enhanced photoluminescence. J Colloid Interface Sci. 2020;565:35–42.

[15] Oluwafemi OS, Sakho EHM, Parani S, Lebepe TC. Fundamentals of quantum dot nanocrystals. Ternary Quantum Dots. 2021;1–34.

[16] Aladesuyi OA, Oluwafemi OS. Synthesis strategies and application of ternary quantum dots — in cancer therapy. Nano-Struct Nano-Objects. 2020;24:100568.

[17] Yang D, Wei X, Piao Z, Cui Z, He H, Wen Z, et al. Constructing bimodal nanoprobe based on Gd:$AgInS_2$/ZnS quantum dots for fluorometric/magnetic resonance imaging in mesenchymal stem cells. J Mater Sci Technol. 2023;148:116–22.

[18] Jose Varghese R, Parani S, Remya VR, Maluleke R, Thomas S, Oluwafemi OS. Sodium alginate passivated $CuInS_2$/ZnS QDs encapsulated in the mesoporous channels of amine modified SBA 15 with excellent photostability and biocompatibility. Int J Biol Macromol. 2020;161:1470–4.

[19] Jiao M, Li Y, Jia Y, Yang Z, Luo X. Aqueously synthesized color-tunable quaternary Cu-In-Zn-S quantum dots for Cu(II) detection via mild and rapid cation exchange. Sens Actuators B Chem. 2019;294:32–9.

[20] Zheng Y, Sadeghimakki B, Brunning JAL, Piano EM, Sivoththaman S. Emission and decay lifetime tunability in less-toxic quaternary ZnCuInS quantum dots. IEEE Trans Nanotechnol. 2021;20:525–33.

[21] Jia L, Wang Y, Nie Q, Liu B, Liu E, Hu X, et al. Aqueous-synthesis of $CuInS_2$ core and $CuInS_2$/ZnS core/shell quantum dots and their optical properties. Mater Lett. 2017;200:27–30.

[22] Mei S, Zhu J, Yang W, Wei X, Zhang W, Chen Q, et al. Tunable emission and morphology control of the Cu-In-S/ZnS quantum dots with dual stabilizer via microwave-assisted aqueous synthesis. J Alloy Compd. 2017;729:1–8.

[23] Ibrahim Y, Meslam M, Eid K, Salah B, Abdullah AM, Ozoemena KI, et al. A review of MXenes as emergent materials for dye removal from wastewater. Sep Purif Technol. 2022;282:120083.

[24] Jlassi K, Eid K, Sliem MH, Abdullah AM, Chehimi MM. Calix[4]arene-clicked clay through thiol-yne addition for the molecular recognition and removal of Cd(II) from wastewater. Sep Purif Technol. 2020;251:117383.

[25] Ibrahim Y, Kassab A, Eid K, Abdullah AM, Ozoemena KI, Elzatahry A. Unveiling fabrication and environmental remediation of mxene-based nanoarchitectures in toxic metals removal from wastewater: Strategy and mechanism. Nanomaterials. 2020;10:885.

[26] Sakthi Priya T, Chen TW, Chen SM, Kokulnathan T. Bismuth molybdate/graphene nanocomposite for electrochemical detection of mercury. ACS Appl Nano Mater. 2022;5:12518–26.

[27] Zhao RX, Liu AY, Wen QL, Wu BC, Wang J, Hu YL, et al. Glutathione stabilized green-emission gold nanoclusters for selective detection of cobalt ion. Spectrochim Acta - Part A Mol Biomol Spectrosc. 2021;254:119628.

[28] Rehman AU, Nazir S, Irshad R, Tahir K, ur Rehman K, Islam RU, et al. Toxicity of heavy metals in plants and animals and their uptake by magnetic iron oxide nanoparticles. J Mol Liq. 2021;321:114455.

[29] Feng RW, Zhao PP, Zhu YM, Yang JG, Wei XQ, Yang L, et al. Application of inorganic selenium to reduce accumulation and toxicity of heavy metals (metalloids) in plants: The main mechanisms, concerns, and risks. Sci Total Env. 2021;771:144776.

[30] Wu X, Li Y, Yang S, Tian H, Sun B. A multiple-detection-point fluorescent probe for the rapid detection of mercury(II), hydrazine and hydrogen sulphide. Dye Pigment. 2020;174:108056.

[31] Pesavento M, Profumo A, Merli D, Cucca L, Zeni L, Cennamo N. An optical fiber chemical sensor for the detection of Copper(II) in drinking water. Sensors. 2019;19:1–13.

[32] Mandegani F, Zali-Boeini H, Khayat Z, Scopelliti R. A smart low molecular weight gelator for the triple detection of copper (II),

mercury (II), and cyanide ions in water resources. Talanta. 2020;219:121237.
[33] Elkhatat AM, Soliman M, Ismail R, Ahmed S, Abounahia N, Mubashir S, et al. Recent trends of copper detection in water samples. Bull Natl Res Cent. 2021;45:45–218.
[34] Muthivhi R, Parani S, May B, Oluwafemi OS. Green synthesis of gelatin-noble metal polymer nanocomposites for sensing of Hg^{2+} ions in aqueous media. Nano-Struct Nano-Objects. 2018;13:132–8.
[35] El Nady J, Ali M, Kamel OA, Ebrahim S, Soliman M. Room temperature synthesis of aqueous ZnCuInS/ZnS quantum dots. J Dispers Sci Technol. 2020;41:1956–62.
[36] Rajendran JV, Parani S, Pillay R, Remya V, Lebepe TC, Maluleke R, et al. Selective and sensitive detection of Cu^{2+}ions in the midst of other metal ions using glutathione capped $CuInS_2$/ZnS quantum dots. Phys E Low-Dimens Syst Nanostruct. 2022;136:115026.
[37] Asadi F, Azizi SN, Chaichi MJ. Green synthesis of fluorescent PEG-ZnS QDs encapsulated into Co-MOFs as an effective sensor for ultrasensitive detection of copper ions in tap water. Mater Sci Eng C. 2019;105:110058.
[38] Liu Y, Zhu Y, Liu X, Dong L, Zheng Q, Kang S, et al. CdSe/ZnS QDs embedded polyethersulfone fluorescence composite membrane for sensitive detection of copper ions in various drinks. J Env Sci Health - Part B Pestic Food Contam Agric Wastes. 2023;58:1–11.
[39] Gong T, Liu J, Liu X, Liu J, Xiang J, Wu Y. A sensitive and selective sensing platform based on CdTe QDs in the presence of L-cysteine for detection of silver, mercury and copper ions in water and various drinks. Food Chem. 2016;213:306–12.
[40] Xiong H, Wang B, Wen W, Zhang X, Wang S. Fluorometric determination of copper(II) by using 3-aminophenylboronic acid-functionalized CdTe quantum dot probes. Microchim Acta. 2019;186:392.